

# Compositional dependence of Ag photodissolution in S-rich ternary As-S-Ge glassy films

D. TSIULYANU\*, I. STRATAN

*Department of Physics, Technical University, bd. Dacia 41, Chisinau MD-2060, Moldova*

The kinetics of the photodissolution of Ag into S - rich As-S-Ge glassy films of various compositions along the tie-line  $(\text{GeS}_4)_x(\text{AsS}_3)_{1-x}$  ( $0 \leq x \leq 1$ ) has been studied by monitoring the changes that occur in their optical transmission of weakly absorbed broadband light. It was shown that the kinetics profiles comprise two consecutive linear steps followed by a quasi – parabolic tail, but the transitions between these steps are not monotonic. The photodissolution rate and the amount of adopted Ag on the first step were found (except of  $\text{GeS}_4$ ) not to depend on glass composition. This result was ascribed to provide evidence for a preferential and direct interaction of Ag with free sulfur at the interface. The rate of photodissolution on the second linear step exhibits a compositional maximum around  $(\text{GeS}_4)_{0.33}(\text{AsS}_3)_{0.67}$ , being by two orders of magnitude higher than the rate for  $\text{GeS}_4$ . The diffusion coefficient, determined from the final quasi-parabolic step of the photodissolution, reaches its maximal value  $k = 3, 5 \cdot 10^{-13} \text{ cm}^2\text{s}^{-1}$  for the same composition, that is  $(\text{GeS}_4)_{0.33}(\text{AsS}_3)_{0.67}$ . The revealed compositional dependences are qualitatively attributed to the fact that only some, very specific glassy compositions being Ag photodoped yield a homogeneous material.

(Received June 20, 2011; accepted August 10, 2011)

*Keywords:* Glassy chalcogenides, Photodissolution, Kinetics

## 1. Introduction

Photodissolution (synonymously called photodoping or photodiffusion) of the metals (e.g. Ag) in chalcogenide glasses (ChG), being to all appearances a unique property of these materials, is widely discussed in the science literature (see an extensive review ref. [1]).

This phenomenon was firstly reported by Kostyshin et al. [2] and has a considerable potential to be applied in high-resolution lithography and Programmable Metallization Cell technologies (reviews ref. [3] and [4] respectively). It was pointed out that photodissolution (PD) process is due both to an inhomogeneous chemical photo-induced reaction, which results in formation of a solid mixture  $\text{ChG}:\text{Ag}$  with a high ionic conductivity (superionic conductor) [5] and diffusion of  $\text{Ag}^+$  ions through this superionic layer [5,6]. The physical mechanism of Ag photodissolution in ChG was explained either in the terms of photochemical reaction due to local heating [7] or combined ionic and electronic charge carrier transport [8]. The last model gives an elegant explanation of the parabolic tail of PD kinetics as well as of origin of the induction period that occurs before the onset of photodissolution proper, and brings to light the reason why the actinic light has to be absorbed at the interface between doped and undoped regions of ChG film. These features of photodissolution process are commonly observed experimentally being controlled by external factors, such as light intensity and wavelength, temperature, pressure etc [1].

Recently, Jain and co-workers [9] have suggested that the PD by mechanism of combined ionic and electronic charge carrier transport, proposed early in [1,8], starts at the interface by chemical reaction between homopolar chalcogen (S-S) segments and neutral Ag forming  $\text{Ag}_2\text{S}$ . Then  $\text{Ag}_2\text{S}$  reacts with “wrong” bonds (such as As-As) converting the neutral silver into  $\text{Ag}^+$  ions, which are able to diffuse deeper in the chalcogenide film.

As all listed mechanisms of PD overlaps, it is not easy to distinguish between them. In this context the compositional features of this phenomenon are of paramount importance. To time, only few investigations are devoted to study the influence of composition on PD process and only binary systems Ge-Ch [10-12] or As-Ch [13-15], (where Ch=S, Se or Te) have been used for this purpose.

The compositional dependences of PD rate and the total amount of photodissolved Ag in glassy  $\text{Ge}_x\text{S}_{1-x}$  ( $21 < x < 45$ ) have been carried out thoroughly by Kawaguchi and Maruno [10]. Their data have shown a high photodiffusion rate of Ag in both S and Ge-rich glasses, with the minimum for composition  $\text{GeS}_2$ , known as composition at which the threshold of elastic and other properties occurs [16, 17]. At the same time, the total amount of silver able to be adopted follows a vice-versa law: S and Ge-rich glasses adopt a relative low amount of Ag, but the maximum of Ag adopts namely  $\text{GeS}_2$ .

However, there are some works [11-12] in which the amount of adopted silver in Ge based ChG was found to be always the same as Ge content, but the amount of silver adopted in As based ChG increases linearly with the

chalcogen (S or Se) content [14,15].

Thus, the effect of backbone composition on photodissolution of metals (e.g. Ag) is still not well understood and further efforts are needed in this context.

In the present work we report the influence of composition of ChG on silver photodissolution process, by transition from threefold coordinated As-based backbone to fourfold coordinated Ge-based structure. Ternary chalcogenide glasses As-S-Ge appeared to be the most attractive for this purpose because their backbone consists of a variety of structural units [18] of a molecular size (including both threefold and fourfold coordinated ones), which are linked to each other at a random network, although the clustering of 10-20 Å are admitted.

We restricted ourselves to the study of a single pseudo-binary system  $\text{GeS}_4$  -  $\text{AsS}_3$  because of following reasons:

1. The glasses over this compositional section are S-enriched and comprise not much different quantities (75-80 at %) of sulphur. The chalcogen (sulphur) enriched glasses are considered the most favourable for photodissolution of Ag, because they yield homogeneous photoreaction products [19].

2. The alteration of composition along this pseudo-binary section allows realization of a monotonous transition from tetrahedral to trigonal connectivity of the network.

3. The photodissolution of Ag in  $\text{GeS}_4$ , which is an extreme composition of this section, is rather well studied [20], and so it appeared attractive spying this process by transition to the second extreme –  $\text{AsS}_3$ .

4. The mean coordination number of glassy alloys of this system ( $\bar{r} = 2.25 \div 2.4$ ) lies below the point of topological transition i.e.  $r = 2.67$  [21] and, following

Tanaka's arguments [17], the structures of all compositions can be considered as only two-dimensional.

## 2. Experimental procedures

The glassy alloys were prepared by melt-quenching method of pure (99, 99%) As, S and Ge in quartz ampoules evacuated up to  $5 \times 10^{-5}$  Torr. The ampoule was rotated around the longitudinal axis at velocity of 7-8 rotations / min and was agitated for homogenization during the synthesis time (24 h). The mixture was melted at 700-1000 °C depending on the composition. The ampoules were then quenched in air. Ampoules containing germanium-enriched alloys were quenched on a copper refrigerator with running water.

Seven compositions, which are listed in Table 1 in the form of  $(\text{GeS}_4)_x(\text{AsS}_3)_{1-x}$ , have been synthesized along the examined compositional section. The ingots could be broken easily showing glassy breaking edges. All glasses with exception of  $\text{GeS}_4$  were clear and homogeneous, their colour changing from orange to yellow. The ingots of  $\text{GeS}_4$  were yellow and smooth.

The chalcogenide thin films have been prepared by thermal "flash" evaporation of priory-synthesized materials onto Pyrex glass substrates, at room temperature. The evaporation was performed from a tantalum boat at the working pressure of  $10^{-4}$  Pa. The thickness of the films was around 1µm and the area of deposition being about 1,5 cm<sup>2</sup>. The silver films were deposited also by thermal evaporation in vacuum on top of the chalcogenide films, immediately (breaking the vacuum) after their preparation. The thickness of the silver film (controlled by equivalent quantity of evaporated Ag) was kept constant of about 50 nm.

Table 1. Composition, concentration of structural units and some physical parameters of  $(\text{GeS}_4)_x(\text{AsS}_3)_{1-x}$  glasses.

Nr	Com. [x]	$E_g$ , eV	Concentration, mol/cm <sup>3</sup> · 10 <sup>-2</sup>			$k \cdot 10^{13}$ , cm <sup>2</sup> s <sup>-1</sup>
			[AsS] <sub>3/2</sub>	[GeS] <sub>4/2</sub>	[SS] <sub>2/2</sub>	
1	0	2.75	1.57	0	1.17	2.80
2	0.17	2.69	1.30	0.26	1.23	2.13
3	0.33	2.66	0.96	0.48	1.2	3.5
4	0.5	2.61	0.69	0.69	1.21	1.42
5	0.67	2.59	0.44	0.88	1.23	0.79
6	0.83	2.56	0.22	1.08	1.24	0.33
7	1	2.54	0	1.22	—	—

The photodissolution of silver onto ChG was performed by illumination the Ag film, lying on the top of the multilayer structure, using the light of a 100 W halogen lamp focused by a quartz lens. Taking into

consideration that the light is reactively absorbed at the photodoped / undoped chalcogenide interface, the exposure was performed from the side of transparent substrate (Fig. 1). The incident power was measured by

vacuum thermoelement VTh-8 (Carl Zeiss, Germany) and was estimated at the sample surface as  $250 \text{ mW/cm}^2$ .

The PD rate was measured by monitoring the changes that occur in the transmittance of the sample of weakly absorbed in ChG broadband probing light as photodissolution proceeds. The optical gaps ( $E_g$ ) of materials in question are listed in Table 1 [22]. Taking into consideration that for all materials  $E_g > 2,54 \text{ eV}$ , the wavelength of the probing light was chosen as  $\lambda > 0.65 \mu\text{m}$  that is in the range of whole transparency of used ChG. For this purpose a cut filter (KC-15) with transparenance range 650-3000 nm was placed behind the sample, i.e. in front of photomultiplier, which served as light detector. A PC with a data acquisition board manufactured by National Instruments Inc. was used for processing. The measurements were carried out at room temperature except of an additional experiment described further in the text.

Fig. 1 shows schematically the multilayer structure of the sample. There are three well-defined boundaries: 1) substrate / undoped ChG; 2) undoped ChG / photodoped material (solid electrolyte); 3) photodoped material / Ag. During the photodissolution the boundary between photodoped material and undoped ChG propagates towards the substrate, but the boundary between photodoped material and Ag propagates in opposite direction i.e. towards surface, so that the thickness of both Ag layer and undoped ChG glass decrease with time.

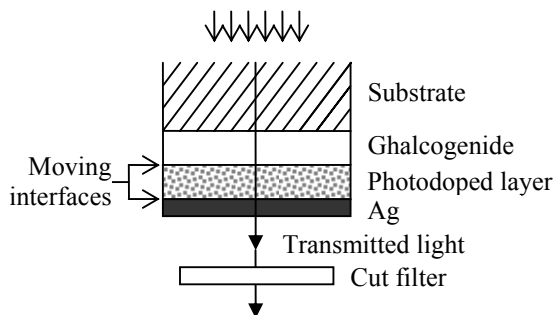


Fig. 1. Schematic cross - section through a sample during the photodissolution process.

In the present work we have tracked the movement of boundary between photodoped material and Ag layer measuring the transmission of weakly absorbed in ChG light with PD of silver in progress.

The instantaneous transmission of unreacted Ag layer ( $T_{Ag}$ ) and that of the whole two-layered ChG / Ag structure ( $T$ ) are interdependent as  $T_{Ag} = T / T_0$ , were  $T_0$  is the transmission of pure ChG layer on glassy substrate. Hence, the PD rate of Ag can be estimated by measuring the recovery rate of optical transmission of two-layer structure ChG / Ag in IR region of spectrum if the thickness dependence of Ag film transmittance is a priori known [23].

### 3. Results

Fig. 2 shows the optical transmission of the two-layered structure ChG / Ag (broadband light  $\lambda > 0.650 \mu\text{m}$ ) versus exposure time as PD proceeds at room temperature. The numbers by each curve correspond to the ChG composition numbers listed in Table 1. The shaded area indicates the transmittance of pure  $(\text{GeS}_4)_x (\text{AsS}_3)_{1-x}$  film, i.e. without Ag layer. It is seen that independently of composition the transmission of two - layer structure in the region of weakly absorbed light, recovers to that of pure ChG, i.e. before deposition of Ag layer. Obviously this is due to a decrease of Ag layer effective thickness: the absorption coefficient of Ag film, is about  $10^5 \text{ cm}^{-1}$  [24], but even high ( $\sim 60 \text{ at. \%}$ ) Ag doped As-S or Ge-S layers are nearly transparent in this region of spectrum [19, 25].

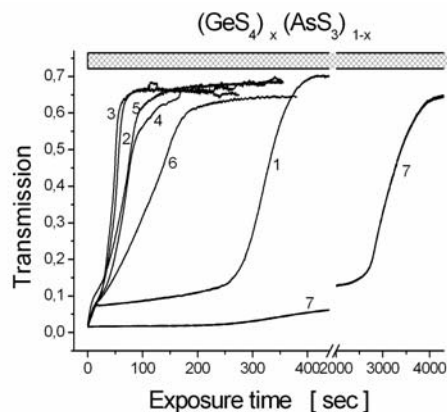


Fig. 2. Transmission of a broadband light  $\lambda > 0.65 \mu\text{m}$  of two-layered structures versus exposure time. The numbers of curves correspond to the composition numbers listed in Table 1. The shaded area indicates the transmittance of pure  $(\text{GeS}_4)_x (\text{AsS}_3)_{1-x}$  films.

Except of  $\text{GeS}_4$ , an induction period was not observed for other compositions in this experiment. On the contrary, a very sharp rising of transmittance was observed at early stage of PD process. Note that the similar behavior, i.e. the high rate of Ag photodissolution could be observed in glassy  $\text{As}_2\text{S}_3$  only at enhanced ( $> 75 \text{ }^\circ\text{C}$ ) temperatures [23]. Further, this fast stage turns into a composition dependent shoulder, followed by a transition to usual monotonic increasing of transmittance as PD proceeds.

We have calculated and plotted the thickness of unreacted Ag film versus exposure time (PD kinetics) applying our experimental data ( $T_{Ag}$ ) to the thickness dependence of transmission spectra of silver films measured by X. Sun et al. [26]. The error of such a method is caused mainly by progressive light absorption in doped layer during PD. The relative error of transmission, being minimal at the beginning of PD process, becomes maximal (about 5 %) closely to its finish. However, the transmission of Ag layer below 20 nm increases very rapidly with decrease of its thickness [26]. Therefore the error in Ag thickness determination below 20 nm, by 5%

error in transmission of unreacted Ag film, is assessed to be of about 1 nm.

Fig. 3 shows the unreacted Ag layer thickness (with displayed error bars) versus exposure time for several compositions of  $(\text{GeS}_4)_x(\text{AsS}_3)_{1-x}$  system. For all compositions, except of  $\text{GeS}_4$ , three stages of PD kinetics can be distinguished clearly: (I) the first, very sharp step is nearly independent on composition but the thickness of Ag layer linearly decreases with exposure time, (II) the second one is a linear shoulder with a slope (the PD rate) strongly influenced by ChG composition and the final (III) step exhibits a weak sub linear dependence of thickness change of Ag layer on time, particularly observed for  $\text{GeS}_4$ .

It should be mentioned that PD of Ag in  $\text{GeS}_4$  was observed in our experiments to exhibit particular behaviour. For one thing, the PD is preceded by a relatively short induction period. Further, it precedes very slowly (Fig. 2 and 3) at all stages: 10-100 times slower than in any other composition in question, and as a consequence, the first sharp step of PD in  $\text{GeS}_4$  does not overlap with similar steps of other compositions.

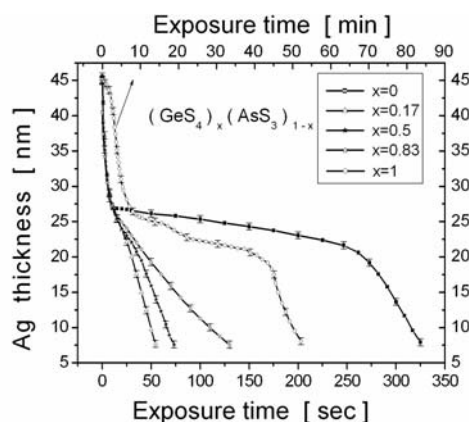


Fig. 3. Decrease of Ag film thickness versus exposure time for several compositions of  $(\text{GeS}_4)_x(\text{AsS}_3)_{1-x}$  system. In order not to overload the picture, the error bars (being identical) are displayed only for several data points.

#### 4. Discussions

The segmentation of kinetics curve (plot of Ag layer thickness change versus time) with non monotonic transition between steps of PD process was reported in our previous paper for glassy  $\text{As}_2\text{S}_3$  [23], which is a binary stoichiometric compound. The PD rate on the first linear step was found for  $\text{As}_2\text{S}_3$  strongly to depend on temperature, but at room temperature it exhibits the value of about 0.5 nm/s.

Fig. 4a shows the PD rate on the first linear step for the glassy materials applied in the present investigation. As one can follow from this figure the PD rate being of about 2.0 nm/s is several times higher than for  $\text{As}_2\text{S}_3$  [23] by the same conditions and, what is more, with except of  $\text{GeS}_4$ , the PD rate does not much vary with glass

composition.

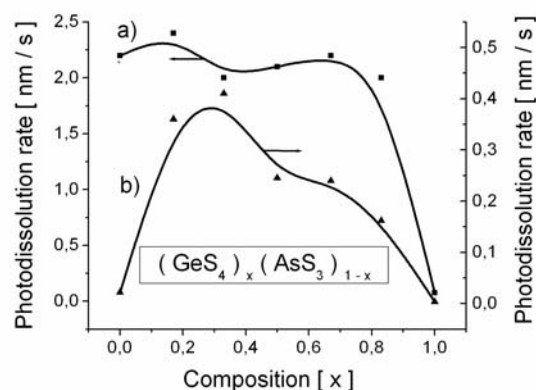


Fig. 4. The photodissolution rate on the first (a) and second (b) linear steps versus glass composition.

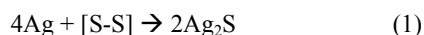
Obviously, this is due to features of multicomponent and / or nonstoichiometric chalcogenide glasses originated from their compositional and structural complexity.

Since early stage of investigation, these materials were treated [27] as an amalgamation of elemental structural units (s.u.) connected in a random network or comprising clusters of a scale of 10-20 Å. The molecular additivity rules have been developed [27, 28], what allow assessing the molar concentration of different s.u., applying the experimentally measured density of the glassy material. This approach appeared to be useful as compositional dependences of some physical properties (microhardness, electrical conductivity, and optical gap et al.) could be understood qualitatively or even calculated quantitatively for different multicomponent glasses [18].

We have applied the additivity rules developed by Muller and co-workers for glassy As-S-Ge system [29] to the compositions  $(\text{GeS}_4)_x(\text{AsS}_3)_{1-x}$ , which are the subject of the present investigation. The s.u. molar concentrations, calculated using material densities taken from [30], are listed in Table 1. It is seen that the concentration of trigonal s.u.  $[\text{AsS}]_{3/2}$  decreases but the concentration of tetrahedral  $[\text{GeS}]_{4/2}$  s.u. increases monotonically. At the same time, the concentration of  $[\text{S-S}]_{2/2}$  s.u. does not vary essentially, that is all glassy materials in question comprise nearly the same concentration of free sulfur. There is no an additivity rule developed to assess the concentration of s.u. in  $\text{GeS}_4$ , but it is well known [20, 31] that this compound also comprises a significant amount of free sulphur in the form of S-chains and  $\text{S}_8$  monomers.

We are conscious that the homogeneous continuous random network description is not a rule and as was shown by Wang and co-workers [32] the phase separation can occur on a macroscopic scale. However, this phenomenon does not exclude the existence of free sulphur in S-rich glasses predicted by continuous random network approach. In this context we assert that namely the availability of free sulphur in all examined glasses, especially in the form of  $[\text{S-S}]$  chains, explains both the

high rate of PD on the first linear step and its weak dependence on composition. In fact, following the model suggested in [9], the silver dissolution starts at the interface by chemical reaction between these segments and neutral Ag as:



The large amount of free sulphur, i.e. [S-S] segments leads to formation of a sufficient amount of  $\text{Ag}_2\text{S}$  to be connected both in  $(\text{Ag}_2\text{S})_x(\text{GeS}_4)_{1-x}$  and  $(\text{Ag}_2\text{S})_x(\text{AsS}_3)_{1-x}$  glasses. As a result the percolation threshold occurs in the layer at the interface along with its transition to superionic conductivity [33]. Not much difference in the concentration of [S-S]<sub>2/2</sub> structural units, i.e. in amount of free sulphur (Table 1), results in overlapping of kinetics curves on the first stage of PD, as well as in their identical length.

As far as particular behaviour of  $\text{GeS}_4$  is concerned, the possibility of formation of Ge-rich material on the interface Ag/ $\text{GeS}_4$  that controls the PD process at high intensities of light irradiation has to be taken into consideration. Such a phenomenon recently has been pointed out by Jin, Boolchand and Mitkova [34] by silver photodissolution in  $\text{Ge}_{30}\text{Se}_{70}$ , which is a Se-rich glassy compound.

By analogy with Ag photodissolution in selenium rich glasses from the system Ge-Se [34, 35], we assume that the solid state reaction of Ag and sulphur rich glasses from the system Ge-S has to be controlled by intensity of applied light. As a matter of fact, the photodissolution of Ag in  $\text{GeS}_4$ , being proceeded at low intensities of light irradiation ( $\sim 4.5 \text{ mW/cm}^2$ ), was found [20] to happen immediately (without an induction period) and the reaction product to be substantially  $\text{Ag}_2\text{S}$ . This case is considered as a milder effect over structure of the host. In the present work, the PD of silver into  $\text{GeS}_4$  was performed applying a much higher intensity of irradiation light ( $\sim 250 \text{ mW/cm}^2$ ) and by analogy with [34] the structure on the interface Ag/ $\text{GeS}_4$  may be different from the structure in the bulk. The last can explain the appearance of an induction period and a very low rate of photodissolution of Ag in  $\text{GeS}_4$ , while the general shape of PD kinetics curve remains the similar to other examined compositions.

The second step of PD kinetics (Fig. 3) shows also a linear dependence of the change of Ag thickness on time (the constant rate of PD), but its slope strongly depends on the glass composition. The variation of PD rate with  $(\text{GeS}_4)_x(\text{AsS}_3)_{1-x}$  composition determined from the slope of the second step is shown in Fig. 4b. As the  $\text{GeS}_4$  content is increased the PD rate increases to a maximum around  $(\text{GeS}_4)_{0.33}(\text{AsS}_3)_{0.67}$  and then falls down. The maximum and minimum rates differ by 20 times if the pure  $\text{GeS}_4$  is not considered. The PD rate in pure  $\text{GeS}_4$  appears to be more than two orders of magnitude (120 times) smaller than the value of this rate at the compositional maximum.

The constant rate of photodissolution is generally agreed to be determined by reaction between metal and ChG, which occurs simultaneously in two different spatial

regions of the sample: (I) absorption of photons by breaking As(Ge)-S bonds, that results in a simultaneous producing of non-bridged chalcogen atoms with a single unpaired electron (dangling bond) and generation of free holes at the doped / undoped interface, and (II) creation of  $\text{Ag}^+$  ions at the Ag / doped ChG interface were photogenerated holes, after the drift through doped layer react with neutral Ag atoms. In turn,  $\text{Ag}^+$  ions after the drift towards the doped / undoped interface accept the unpaired electron from chalcogen dangling bond and a photodoped quaternary Ag-As-S-Ge compound is created. Thus, the reaction limited stage of PD depends either on electronic (hole) photoconductivity of doped layer  $\sigma_{ph}$  or on its ionic conductivity  $\sigma_{\text{Ag}^+}$ .

Investigation of the effect of temperature on the PD kinetics allows [23] in principle to distinguish between effects of photoconductivity  $\sigma_{ph}$  and ions conductivity  $\sigma_{\text{Ag}^+}$  of doped layer on reaction rate. For this purpose the effect of temperature on Ag photodissolution was checked for  $(\text{GeS}_4)_{0.67}(\text{AsS}_3)_{0.33}$ , which is a composition arbitrary chosen from the examined glassy alloys.

Fig. 5 illustrates the photoreaction rate of this composition estimated from the second step of PD kinetics versus temperature in Arrhenius coordinates.

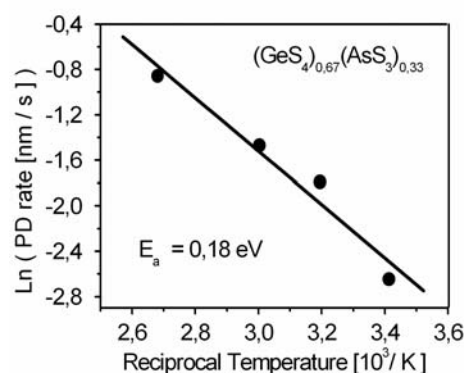


Fig. 5. Temperature dependence of PD rate on the second (b) stage plotted in Arrhenius coordinates. The line is drawn as guides to the eyes.

The slope of this line exhibits a relatively low value of activation energy (0.18 eV), which is usually ascribed to photoconductivity [5, 6, 23] of Ag-doped layer. Thus, we assert that the PD kinetics on the second step is a reaction limited process by photoconductivity  $\sigma_{ph}$  under condition that  $\sigma_{ph} \ll \sigma_{\text{Ag}^+}$ .

The final (third) step of PD kinetics reveals the dual behaviour. The thickness of Ag film being plotted versus either exposure time or square-root of exposure time shows (with exception of  $\text{GeS}_4$ ) linear dependences. We assert that the reason for such behaviour is the high speed of PD making the process to occur on the beginning of parabolic curve, which is nearly a line. As it is not possible

unambiguity to turn out the relation describing the last step of PD we have considered the both versions.

If the linear version is considered, the compositional dependence of photoreaction rate can be revealed. Fig. 6 shows the PD rate on the third step versus glass composition, except of  $\text{GeS}_4$ .

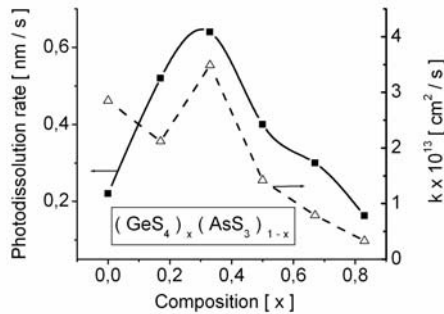


Fig. 6. Compositional dependences of photoreaction rate and photodiffusion coefficient  $k$  revealed from the third step of PD kinetics.

Again a maximum around composition  $(\text{GeS}_4)_{0.33}(\text{AsS}_3)_{0.67}$  is observed, the maximum and minimum rates differing by a factor of about 3.

Considering the quasi-parabolic version, the thickness change of Ag layer was plotted as a function of square root of exposure time for different compositions related to the last step of PD kinetics (Fig. 7). One can see that each curve (except of  $\text{GeS}_4$ ) is a straight line that characterizes a diffusion controlled process. Such a PD process is consistent with model [8] wherein both ionic and electronic charge transport occur simultaneously by the condition that the flux of ions  $j_{\text{Ag}^+}$  balances that of holes

$j_h$  in reverse direction:

$$j_{\text{Ag}^+} = -j_h \quad (2)$$

Each curve from Fig. 7 can be described by relation:

$$\Delta d_t = (2kt)^{\frac{1}{2}} \quad (3)$$

The values of parabolic constant ( $k$ ), estimated from the slope of these curves, are listed in Table 1 and additionally are plotted in Fig. 6 versus glass composition.

One can see that the values of the coefficient  $k$  are in the range of  $(0.33 - 3.5) \cdot 10^{-13} \text{ cm}^2\text{s}^{-1}$  reaching the maximal value for composition  $(\text{GeS}_4)_{0.33}(\text{AsS}_3)_{0.67}$ .

Thus, the photodissolution rate on the both second and third steps of PD kinetics, as well as the diffusion coefficient are highly influenced by the glass composition showing the maximum around the  $(\text{GeS}_4)_{0.33}(\text{AsS}_3)_{0.67}$ .

This is a rather unexpected result as density and mean coordination number [30], optical gap and other physical parameters of  $(\text{GeS}_4)_x(\text{AsS}_3)_{1-x}$  glasses (Table 1) vary monotonically with composition. The appearance of a compositional maximum is probably due to macroscopic

phase separation, which occurs by Ag photodissolution in chalcogen rich glasses [32]. Sometimes, when Ag is alloyed with chalcogenide glasses by melt quenching, thermo or photodiffusion a homogeneous material can be obtained even inside of one class of materials [13].

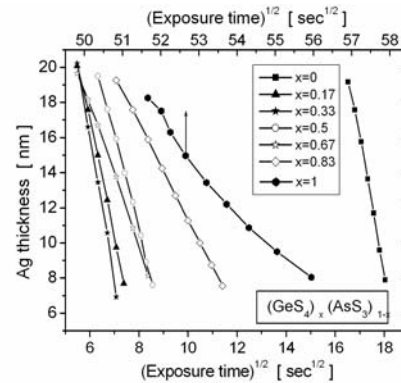


Fig. 7. Decrease of silver thickness vs. exposure time at third (quasi - parabolic) step of PD for different compositions of  $(\text{GeS}_4)_x(\text{AsS}_3)_{1-x}$  system.

We assert that the maxima of both photodissolution rate and of diffusion coefficient around composition  $(\text{GeS}_4)_{0.33}(\text{AsS}_3)_{0.67}$  may be due to the change in the morphology of this glassy material i.e. its homogenization. A homogeneous backbone promotes the transport of both electrons and ions involved in photoreaction because of lack of phase boundaries and additional defects.

## 5. Conclusions

The photodissolution (PD) kinetics of Ag in glassy  $(\text{GeS}_4)_x(\text{AsS}_3)_{1-x}$  films has been studied over a wide composition range ( $0 \leq x \leq 1.0$ ) using optical transmission measurement.

The kinetics profiles comprise two consecutive linear steps followed by a quasi-parabolic tail. The slope of the first very sharp step (the rate of PD  $\sim 2 \text{ nm/s}$ ) does not depend on composition. This step is ascribed to direct interaction of Ag with free sulphur of glassy material at the interface.

The rate of PD on the second linear step, ascribed to photoconductivity limiting solid-state reaction, shows a maximum around  $(\text{GeS}_4)_{0.33}(\text{AsS}_3)_{0.67}$ . At the same composition the diffusion coefficient determined from the quasi-parabolic tail reaches its maximal value of about  $3.5 \cdot 10^{-13} \text{ cm}^2/\text{s}$ . It is assumed that this composition yields a homogeneous reaction product.

Showing an induction period the photodissolution of Ag in  $\text{GeS}_4$  occurs by around two orders of magnitude slower than in other studied compositions, what is predicted to be caused by the phase separation induced by high power light irradiation ( $250 \text{ mW/cm}^2$ ) applied in the present work.

### Acknowledgements

This work was partially supported by SCSTD of Academy of Sciences of Moldova, project 11.817.05.21A.

### References

- [1] A. V. Kolobov, S. R. Elliott, *Adv. Physics* **40**, 625 (1991).
- [2] M. T. Kostyshin, E. U. Mikhailovskya, P. F. Romanenko, *Sov. Phys. (Solid State)* **8**, 451 (1966).
- [3] D. Tsiulyanu, in: *Non-Crystalline Materials for Optoelectronics*, edited by G. Lucovsky and M. Popescu, *Optoelectronic Materials and Devices*, Vol. 1 (INOE Publishing House, Bucharest, (2004) chap.10.
- [4] M. Mitkova, M. N. Kozicki, in: *Non-Crystalline Materials for Optoelectronics*, edited by G. Lucovsky and M. Popescu, *Optoelectronic Materials and Devices*, Vol. 1 (INOE Publishing House, Bucharest, 2004) chap.8.
- [5] J. Ploccharski, J. Przulski and M. Teodorczyk, *J. Non-Cryst. Solids* **93**, 303 (1987).
- [6] A. V. Kolobov, S. R. Elliott, M. A. Taguirdzhanov, *Philos. Mag.* **B61**, 859 (1990).
- [7] J. C Phillips, *J. Non-Cryst. Solids* **64**, 81(1984).
- [8] S. R. Elliott, *J. Non-Cryst. Solids* **130**, 85 (1991).
- [9] H. Jain, A Kovalskiy, A. Miller, *J. Non-Cryst. Solids* **352**,562(2006).
- [10] T. Kawaguchi, S. Maruno, *J. Appl. Phys.* **71**, 2195 (1992).
- [11] J. H. S. Rennie, S. R. Elliott, C. Jeynes, *Appl. Phys. Lett.* **48**, 1430 (1986).
- [12] J. M. Oldale, S. R. Elliott, *J. Non-Cryst. Solids* **128**, 255 (1991).
- [13] P. J. S. Ewen, A. Zakery, A. P. Firth, A. E. Owen, *J. Non-Cryst. Solids* **97-98**, 1127(1987).
- [14] M. Yamaguchi, I. Shimizu and E. Inoue, *J. Non-Cryst. Solids* **47**, 341 (1982).
- [15] T. Wagner, M. Frumar, *J. Non-Cryst. Solids* **116**, 269 (1990).
- [16] D. Tsiulyanu, A. D. Dragich, N. A. Gumeniuk, *J. Non-Cryst. Solids* **155**, 180 (1993).
- [17] K. Tanaka, *Phys. Rev.* **B39**, 1270 (1989).
- [18] R. Andreichin, M. Nikiforova, E. Scordeva, L. Yurukova, R. Grigorovici, R. Manaila, M. Popescu, A. Vancu, *J. Non-Cryst. Solids* **20**, 101 (1976).
- [19] T. Wagner, *J. Optoelectron. Adv. Mater.* **4**, 717 (2002).
- [20] M. Mitkova, M. N. Kozicki, H. C. Kim, T. L. Alford, *Thin Solid Films* **449**, 248 (2004).
- [21] H. He, M. F. Thorpe, *Phys.Rev. Lett.* **54**, 2107 (1985).
- [22] D. Tsiulyanu, N. A. Gumenyuk, *J. Appl. Spectroscopy* **52**, 625 (1990).
- [23] D. Tsiulyanu, I. Stratan, *J. Non-Cryst. Solids* **356**, 147 (2010).
- [24] I. An, H. Oh, *Journ. Korean Phys. Society* **29**, 370 (1996).
- [25] T. Kawaguchi, S. Maruno, S. R. Elliott, *J. Appl. Phys.* **79**, 9096 (1996).
- [26] X. Sun, R. Hong, H. Hou, Z. Fan, J. Shao, *Thin Solid Films* **515**, 6962 (2007).
- [27] R. L. Myuller, in: *Solid State Chemistry*, edited by Z.U. Borisova, (Consultants Bureau, New York, 1966), 1-45.
- [28] R. L. Myuller, V. N. Timofeeva, Z. U. Borisova, in: *Solid State Chemistry*, edited by Z. U. Borisova, (Consultants Bureau, New York, 1966), pp. 46-49.
- [29] R. L. Myuller, G. M. Orlova, V. N. Timofeeva, G. I. Ternovaia, *Vestnik Leningrad. Univ, Seriya Fiz. i Khim.* **22**, 146 (1962) (in Russian).
- [30] D. Tsiulyanu, N. Gumenyuk, S. Marian, *Bul. Acad. Science of Moldova, Seriya Fiz. Tech.*, **3**, 19 (1995).
- [31] X. Feng, W.J. Bresser, P. Boolchand, *Phys. Rev. Lett.* **78**, 4422 (1997).
- [32] Y. Wang, M. Mitkova, D. G. Georgiev, S. Mamedov, P. Boolchand, *J. Phys.: Condensed matter.* **15**, S1573 (2003).
- [33] V. Balan, A. Piarristeguy, M. Ramonda, A. Pradel, M. Ribes, *J. Optoelectr. Adv. Mater.* **8**, 2112 (2006).
- [34] M. Jin, P. Boolchand, M. Mitkova, *J. Non-Cryst. Solids*, **354**, 2719 (2008).
- [35] M. Mitkova, M. N. Kozicki, H. C. Kim, T. L. Alford, *J. Non-Cryst Solids*, **338-340**, 552 (2004).

\*Corresponding author: [tsiu@molddata.md](mailto:tsiu@molddata.md)